

was removed under reduced pressure. The brown oil residue was then poured into diethyl ether (20 mL). Insoluble TEAP was filtered off and the filtrate was evaporated under reduced pressure, at 30 °C. Flash chromatography of the residue on silica gel afforded the expected 1,4-benzoxazine derivative.

**16:** A mixture of 2,2-diphenylacetaldehyde, 2-methoxyethylamine (slight excess), and toluene-*p*-sulfonic acid (catalytic amount) was heated at reflux in benzene for 18 h. The water was removed initially by means of a Dean–Stark separator, and then by using a molecular sieve. The solvent was removed under reduced pressure and the residue distilled. The freshly distilled enamine **A** (2.5 mmol) was dissolved in methanol (250 mL) that contained TEAP as the supporting electrolyte (5 mmol). 3,4-Aminophenol **1<sub>red</sub>** (0.5 mmol) was then added to the resulting solution, along with 2-methoxyethylamine (0.5 mmol). The addition of the latter was necessary to produce the monoanionic species of **1<sub>red</sub>**, which is the sole form that can be oxidized to *o*-azaquinone **1<sub>ox</sub>**.<sup>[5]</sup> The resulting solution was then oxidized, under nitrogen, at room temperature, at a mercury pool whose potential was fixed at +50 mV vs. SCE. After exhaustive electrolysis (4 h, 2.1 Faraday mol<sup>-1</sup>), the solution was treated as above (general procedure) to give the 1,4-benzoxazine derivative **16** in 51 % yield.

**2:** M.p. 133 °C; <sup>1</sup>H NMR (300 MHz, CDCl<sub>3</sub>): δ = 0.85 (d, *J* = 6 Hz, 3 H), 0.90 (d, *J* = 6 Hz, 3 H), 1.25 (s, 3 H), 1.30 (s, 3 H), 1.70 (m, *J* = 6 Hz, 1 H), 1.90 (s, 1 H), 2.50 (m, 1 H), 2.80 (m, 1 H), 4.00 (s, 1 H), 4.65 (s, 1 H), 6.40 (d, *J* = 9 Hz, 1 H), 7.00 (d, *J* = 9 Hz, 1 H), 7.50 (m, 3 H), 7.65 (m, 2 H), 12.8 (s, 1 H); <sup>13</sup>C NMR (75 MHz, CDCl<sub>3</sub>): δ = 20.3, 24.5, 26.3, 28.8, 50.2, 53.0, 92.9, 108.5, 112.6, 120.9, 124.0, 128.0, 128.8, 131.2, 138.4, 146.9, 152.0, 198.5; UV/Vis (methanol): λ<sub>max</sub> (ε) = 258 (21 850), 320 (17 150); MS-DCI: *m/z*: 355 [MH<sup>+</sup>].

**10:** M.p. 110 °C; <sup>1</sup>H NMR (300 MHz, CDCl<sub>3</sub>): δ = 1.25 (s, 3 H), 1.30 (s, 3 H), 2.10 (s, 1 H), 2.90 (dd, *J* = 6 Hz and *J* = 13 Hz, 1 H), 3.10 (dd, *J* = 6 Hz and *J* = 13 Hz, 1 H), 3.35 (s, 6 H), 4.00 (s, 1 H), 4.45 (t, *J* = 6 Hz, 1 H), 4.70 (s, 1 H), 6.40 (d, *J* = 9 Hz, 1 H), 7.00 (d, *J* = 9 Hz, 1 H), 7.50 (m, 3 H), 7.65 (m, 2 H), 12.70 (s, 1 H); <sup>13</sup>C NMR (75 MHz, CDCl<sub>3</sub>): δ = 24.5, 26.3, 47.1, 50.2, 53.4, 54.1, 92.5, 104.2, 108.5, 112.8, 121.0, 123.9, 128.1, 128.9, 131.2, 138.5, 147.1, 152.1, 201.0; UV/Vis (methanol): λ<sub>max</sub> (ε) = 258 (21 670), 319 (17 050); MS-DCI: *m/z*: 387 [MH<sup>+</sup>].

**16:** M.p. 190 °C; <sup>1</sup>H NMR (300 MHz, CDCl<sub>3</sub>): δ = 2.50 (s, 1 H), 3.00 (m, 1 H), 3.10 (m, 1 H), 3.20 (s, 3 H), 3.35 (t, *J* = 6 Hz, 2 H), 5.20 (s, 1 H), 5.80 (s, 1 H), 6.35 (d, *J* = 9 Hz, 1 H), 6.95 (d, *J* = 9 Hz, 1 H), 7.20 to 7.55 (m, 13 H), 7.65 (m, 2 H), 12.90 (s, 1 H); <sup>13</sup>C NMR (75 MHz, CDCl<sub>3</sub>): δ = 45.0, 58.6, 62.4, 72.6, 89.7, 108.8, 112.8, 120.8, 124.6, 126.6, 126.9, 127.0, 128.1, 128.2, 128.4, 128.9, 131.3, 143.0, 144.3, 147.2, 152.3, 200.6; UV/Vis (methanol): λ<sub>max</sub> (ε) = 258 (21 950), 319 (17 200); MS-DCI *m/z*: 481 [MH<sup>+</sup>].

Received: August 27, 2001

Revised: December 14, 2001 [Z17799]

- [1] *Naturally Occurring Quinones IV: Recent Advances*, 4th ed. (Ed.: R. H. Thomson), Blackie, London, **1997**, p. 746.
- [2] For a recent review on the synthesis of quinones, see: W. M. Owton, *J. Chem. Soc. Perkin Trans. 1* **1999**, 2409–2420, and references therein.
- [3] A. A. Kutayev, *Tetrahedron* **1991**, 47, 8043–8065.
- [4] a) M. Largeron, M.-B. Fleury, *Tetrahedron Lett.* **1998**, 39, 8999–9002; b) M. Largeron, B. Lockhart, B. Pfeiffer, M.-B. Fleury, *J. Med. Chem.* **1999**, 42, 5043–5052; c) M. Largeron, B. Mesples, P. Gressens, R. Cecchelli, M. Spedding, A. Le Ridant, M.-B. Fleury, *Eur. J. Pharmacol.* **2001**, 424, 189–194.
- [5] M. Largeron, M.-B. Fleury, *J. Org. Chem.* **2000**, 65, 8874–8881.
- [6] Recently, the metal ion complex of TTO model cofactor was shown to oxidize not only benzylamine but also aliphatic amines in anhydrous organic media, whereas no reaction takes place in the absence of metal ion; see: S. Itoh, M. Taniguchi, N. Takada, S. Nagatomo, T. Kitagawa, S. Fukuzumi, *J. Am. Chem. Soc.* **2000**, 122, 12087–12097.
- [7] For recent reviews on the hetero Diels–Alder reaction, see a) K. A. Jørgensen, *Angew. Chem.* **2000**, 112, 3702–3733; *Angew. Chem. Int. Ed.* **2000**, 39, 3558–3588, and references therein; b) M. Behforouz, M. Ahmadian, *Tetrahedron* **2000**, 56, 5259–5288, and references therein; c) P. Buonora, J.-C. Olsen, T. Oh, *Tetrahedron* **2001**, 57, 6099–6138, and references therein.

- [8] a) H. W. Heine, B. J. Barchiesi, E. A. Williams, *J. Org. Chem.* **1984**, 49, 2560–2565; b) H. W. Heine, M. G. La Porte, R. H. Overbaugh, E. A. Williams, *Heterocycles* **1995**, 40, 743–752, and references therein; c) K. C. Nicolaou, Y. L. Zhong, P. S. Baran, *Angew. Chem.* **2000**, 112, 636–639; *Angew. Chem. Int. Ed.* **2000**, 39, 622–625; d) K. C. Nicolaou, K. Sugita, P. S. Baran, Y. L. Zhong, *Angew. Chem.* **2001**, 113, 213–216; *Angew. Chem. Int. Ed.* **2001**, 40, 207–210.
- [9] D. N. Nicolaides, C. Bezergiannidou-Balouetsi, R. W. Awad, K. E. Litinas, E. Malanidou-Xenikaki, A. Terzis, C. P. Raptopoulou, *J. Org. Chem.* **1997**, 62, 499–502, and references therein.
- [10] a) G. A. Berchtold, J. Ciabattini, A. A. Tunick, *J. Org. Chem.* **1965**, 30, 3679–3681; b) S. Danishefsky, R. Cavanaugh, *J. Org. Chem.* **1968**, 33, 2959–2965, and references therein; c) D. L. Boger, *Tetrahedron* **1983**, 39, 2869–2939, and references therein; d) M. S. South, T. L. Jakubowski, M. D. Westmeyer, D. R. Dukeshner, *J. Org. Chem.* **1996**, 61, 8921–8934; e) S. Turchi, R. Nesi, D. Giomi, *Tetrahedron* **1998**, 54, 1809–1816; f) J. Koyama, I. Toyokumi, K. Tagahara, *Chem. Pharm. Bull.* **1998**, 46, 332–334, and references therein.
- [11] It is known that secondary alkylamines are thermodynamically unstable at room temperature and that the imino form is the only detectable species; see: B. De Jeso, J.-C. Pommier, *J. Chem. Soc. Chem. Commun.* **1977**, 565–566, and references therein.

## Voltage-Driven Changes in Molecular Dipoles Yield Negative Differential Resistance at Room Temperature\*\*

Yoram Selzer,\* Adi Salomon, Jamal Ghabboun, and David Cahen\*

The effect of negative differential resistance (NDR), discovered by Esaki<sup>[1]</sup> in Ge *p*–*n* diodes, forms the basis for a variety of high-speed semiconductor devices.<sup>[2]</sup> As future generations of electronics may rely on molecules as part of intelligent and/or nanoscopic devices,<sup>[3]</sup> much attention is given to the idea of molecular NDR. Experimentally only a few NDR devices utilizing molecules as the active component, have been reported.<sup>[4–10]</sup> Except for one,<sup>[10]</sup> all were effective only at low temperature (*T* < 78 K) and under high-vacuum conditions. Herein we report molecule-controlled, room-temperature NDR in a metal/molecular layer/semiconductor diode in ambient atmosphere.

The diodes use a series of relatively simple molecules of the type depicted in Figure 1. Hg was used as the metal and *p*-Si as the semiconductor because:

- 1) Disulfide molecules are electrochemically active once adsorbed on Hg.<sup>[11]</sup>

[\*] Dr. Y. Selzer, Prof. D. Cahen, A. Salomon, J. Ghabboun  
Department of Materials & Interfaces  
Weizmann Institute of Science  
Rehovot 76100 (Israel)  
Fax: (+972) 8-934-4139  
E-mail: yus1@email.psu.edu, david.cahen@weizmann.ac.il

[\*\*] We thank Prof. D. Mandler (HU Jerusalem) for making the hanging Hg drop electrode available to us, Prof. A. Shanzer and Ms. R. Lazar for synthesizing and providing the cyclic disulfide molecules, and Prof. J. M. L. Martin (all from the Organic Chemistry department, WIS), for guidance with the dipole moment calculations. We thank the Israel Science Foundation for partial support. Y.S. thanks the Clor fund for a postdoctoral fellowship.

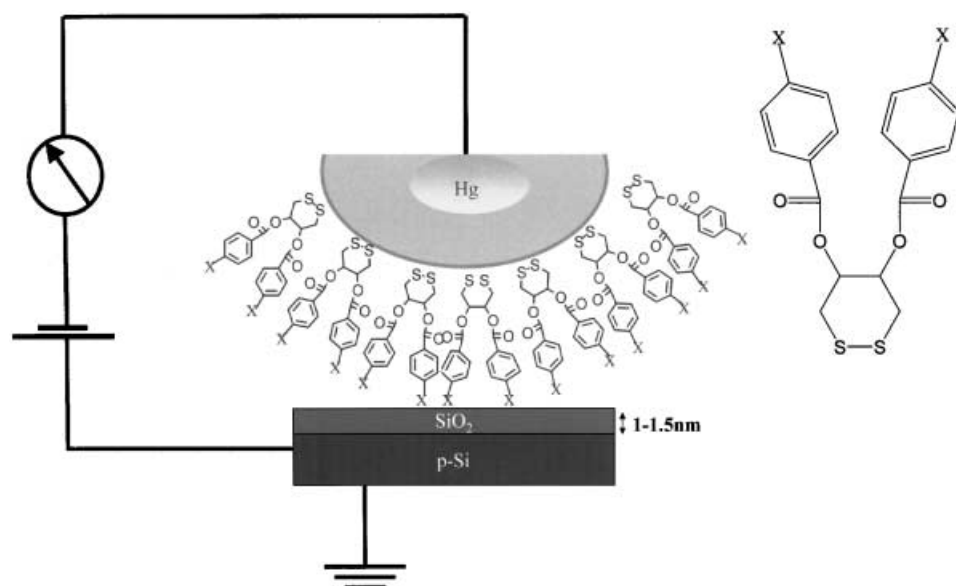


Figure 1. A schematic picture of the junction, and the dipolar molecules used. X = CF<sub>3</sub>, CN, H, OMe.

- 2) Hg can be applied simply as a top contact to relatively large molecular junctions.<sup>[12–15]</sup>
- 3) Hg is known not to react with Si and SiO<sub>x</sub> surfaces.<sup>[16]</sup>
- 4) Hg makes a blocking contact with p-Si.

Junctions were assembled using clean-room facilities and modifying various stages from previously reported procedures.<sup>[12–15]</sup> Characterization of the molecular monolayers used here, which included ellipsometry on Au, were reported by us earlier.<sup>[17]</sup> A typical set of experimental current–voltage (*I*–*V*) curves is shown in Figure 2. The largest NDR was measured for molecules with a CF<sub>3</sub> end group. Such devices had a peak current density > 2 A cm<sup>–2</sup>, NDR < –490 μΩ m<sup>2</sup>, and a peak to valley ratio of 25:1, the best room-temperature NDR characteristics reported for a molecule-based device.

The effect of the other dipoles on *I*–*V* curves is less pronounced, with NDR decreasing as the substituents on the molecules change from CF<sub>3</sub> to CN to H to CH<sub>3</sub>O. We postulate that the observed trend is a result of two contributions, namely, different Schottky barrier heights and voltage driven change in charge transmission.

**Different Schottky barrier heights:** Similar to what we have reported on earlier,<sup>[18–20]</sup> the potential across Schottky junctions can be tuned by assembling monolayers made up of molecules with different dipole moments at the interface. The change in potential is manifested as a change in the barrier height inside the semiconductor,  $\Phi_b$ . This dipole effect is demonstrated here for the first time on a p-type semiconductor. To a first approximation, the barrier height of a

p-type semiconductor is given by [Eq. (1)],<sup>[21]</sup> where  $E_g$  is the band gap of the semiconductor,  $\chi_{sc}$  is its electron affinity,  $\Phi_m$  is the work function of the metal (prior to modification) and  $\Phi_{dipole}$  is the electrostatic potential step associated with the film of molecular dipoles.

$$\Phi_b = E_g + \chi_{sc} - (\Phi_m + \Phi_{dipole}) \quad (1)$$

A dipole layer that effectively increases the metal's work function should decrease the barrier height, after contact is made with a semiconductor. The opposite effect is expected if the dipole layer decreases the metal's work function. The experimental results (see insert of Figure 2, and Table 1) support this: junctions

containing molecules with dipoles for which  $\Phi_{dipole} > 0$ , that is, with CF<sub>3</sub> or CN substituents, have a lower effective barrier height than those with molecules, containing –H or –CH<sub>3</sub>O substituents, for which  $\Phi_{dipole} < 0$ . Samples without molecules

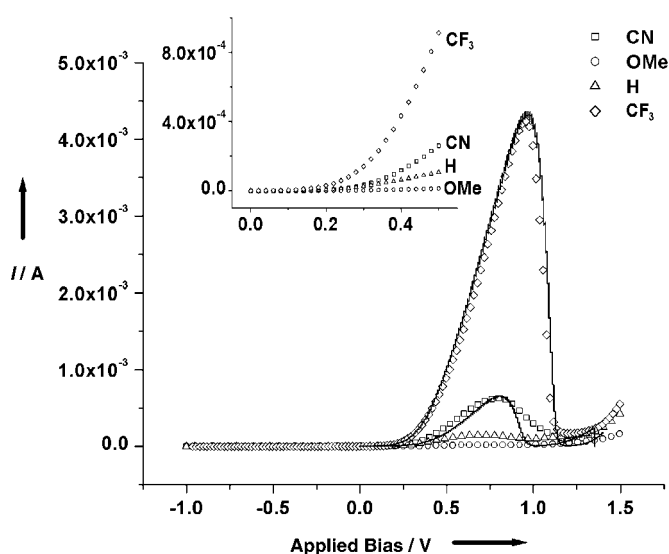


Figure 2. Experimental *I*–*V* curves for junctions of Figure 1, with the different dipolar molecules. For the sake of clarity simulated results (continuous lines) are shown only for the junctions with CF<sub>3</sub>- and CN-substituted molecules. Insert: The low voltage (pre-NDR) range, of the *I*–*V* curves, which shows the effect of the molecular dipole moments on the barrier height of junctions, as described in detail in refs. [18–20].

Tabelle 1. Parameters extracted from *I*–*V* curves and related data. Dipole values were calculated by ab initio methods.  $\Phi_b$  and  $V^{NDR}$  were extracted from the experimental curves.  $\Delta$  and  $V^0$  were the fitting parameters (see text).

End group	Dipole moment [D] <sup>[a]</sup>	$\Phi_b$ [V]	$\Delta$ [eV]	$V^0$ [V]	$V^{NDR}$ [V]	Anion dipole moment [D] <sup>[a]</sup>
CF <sub>3</sub>	0.9	0.36	2.70	0.80	0.92	–1.1
CN	0.4	0.38	1.50	0.60	0.80	–13.4
H	–5.4	0.40	0.95	0.43	0.71	–15.9
CH <sub>3</sub> O	–6.6	0.44	0.45	0.43	0.70	–16.6

[a] Negative dipole values are used to describe dipoles having their negative pole pointing to the metal surface.

do not show NDR and give  $I-V$  curves with higher currents because of the lack of a molecular layer (cf. ref. [18]).

**Voltage driven change in charge transmission:** NDR behavior in our system depends critically on that, upon adsorption on Hg, the cyclic disulfide end of the molecules can undergo a redox reaction [Eq. (2)].<sup>[11]</sup>



Several control experiments verified that indeed the disulfide bond is the electrochemically active part of the molecules:

- 1) Junctions made with simple thiols adsorbed on mercury did not show NDR behavior.
- 2) Cyclic disulfide molecules with long alkyl chains instead of benzene rings showed NDR behavior (see below); thus, the active part of the system is not one of the rings.
- 3) The same dipole molecules adsorbed on gold do not show NDR behavior,<sup>[19]</sup> in agreement with literature data that suggest that disulfide bonds are broken upon their adsorption on gold.<sup>[22]</sup>

The junctions that we deal with are between a metal and a p-type semiconductor which means that under forward bias conditions the Hg atoms are negative with respect to the Si ones. As the forward bias voltage is increased it reaches a value that is sufficiently negative (with respect to the Si) to drive the reduction in Equation (2). This reaction can occur at the interface as no other reagents are needed, there are no products to be removed, and because the necessary electrostatic screening, normally provided by solvent molecules or counterions, is supplied by image charges on the metal.

The two added electrons are mainly localized on the sulfur atoms.<sup>[23]</sup> This localization results from:

- 1) The electronegativity of sulfur.
- 2) That the reduced disulfide bond is not conjugated to the rest of the molecule.
- 3) There is good screening of the disulfide bond by the metal (see above).

As one side of the interface is a semiconductor, extra charge at the interface will normally lead to realignment of the semiconductor energy-band positions, with respect to the metal Fermi level, to change the band bending and thus produce a new barrier height,  $\Phi_b$ , inside the semiconductor. However, since in our case (see Table 1), the reduction in Equation (2) occurs at forward bias potentials that are higher than the barrier height, that is, with no depletion left in the semiconductor, it is likely that the observed NDR results from a change in tunneling probability, rather than from a change in  $\Phi_b$ .

The localized charges reduce the charge transmission across the junction by creating a potential barrier at the ends of the molecules.<sup>[24–27]</sup> Electrons essentially have to tunnel through this potential barrier that can be as high as a few eV. As more molecules are reduced, charge transmission becomes less efficient and the  $I-V$  curve collapses to a curve with lower current characteristics, establishing the NDR effect.

We have semi-quantitatively simulated this process assuming that:

- 1) The governing mechanism of charge transfer in our devices is thermionic emission.<sup>[2]</sup>

- 2) The reaction in Equation (2), the process by which the dipoles are changed, can be treated using Laviron's methodology for surface-bound electrochemical reactions.<sup>[28]</sup>
- 3) Since the molecules are not conjugated, with a free-molecule HOMO–LUMO gap in the order of 7 eV,<sup>[23, 29]</sup> tunneling is assumed to be nonresonant with, as a first approximation, the tunneling probability defined for a rectangular potential barrier.<sup>[2]</sup> The width of the barrier was taken as 2.5 nm, based on ellipsometry measurements of the SiO<sub>2</sub> (1.5 nm) and of the molecular monolayers (1 nm, see reference [17]).

Fitting of simulations could be carried out by varying only two parameters, the maximal change in tunneling barrier,  $\Delta$ , and  $V^0$  the “standard reduction potential” of the disulfides. The barrier height,  $\Phi_b$ , and  $V^{\text{NDR}}$ , the onset potential of NDR were extracted from the experimental curves.<sup>[30]</sup>

The different parameters are summarized in Table 1. From this we see that:

- 1) There is excellent qualitative agreement between the trend seen in the onset potentials of NDR (calculated by differentiating the  $I-V$  curves) and the standard redox potentials,  $V^0$ , of Equation (2) that were used as fitting parameters. The onset potentials are shifted relative to the  $V^0$  values, because of the irreversibility of the reduction process.<sup>[28]</sup>
- 2) The added barrier for tunneling correlates well with the calculated dipoles for the anions that are produced by reduction in Equation (2). Internal electrostatic fields are known to affect the rates of charge transfer.<sup>[31, 32]</sup> In general, electron transfer in the direction of a permanent dipole ( $\delta^+ \rightarrow \delta^-$ ) is slower than the rate of electron transfer in a direction that opposes the dipole. In our case, the molecules with the electron withdrawing groups, that is, CF<sub>3</sub> and CN, have the highest opposing field to electron transfer from the Hg to the p-Si. The dipole with the CF<sub>3</sub> substituent produces the strongest NDR because this dipole produces the biggest change in junction properties, that is, from initial smallest Schottky barrier to final lowest tunneling probability (see Table 1).

The devices age as a consequence of repeated cycling and the NDR effect usually disappears after 3–4 cycles.<sup>[33]</sup> This effect is probably because of complete random disorientation of the molecules after detachment from the mercury following reduction [Eq. (2)]. Structural rearrangements at interfaces have been shown to exist even in highly ordered monolayers.<sup>[34]</sup> Rearrangements at our interfaces are probable because the molecules used are too short to allow their assembly into highly ordered monolayers. Indeed, we know from previous studies that layers of this type of disulfide molecules are not highly ordered.<sup>[17]</sup> To test this, we made a device based on a similar molecule with long alkyl chains instead of the benzene rings. This molecule, monolayers of which on Au were found to be twice as thick (2 nm) as those of the molecules shown in Figure 1 (1 nm<sup>[17]</sup>) gives a more ordered monolayer than the other cyclic disulfide species used here.<sup>[17]</sup> The resulting  $I-V$  curves in Figure 3 show that after several cycles the junction becomes stable without any further degradation. Initial aging probably results from some structural rearrangements in the vicinity of defects in the monolayer.

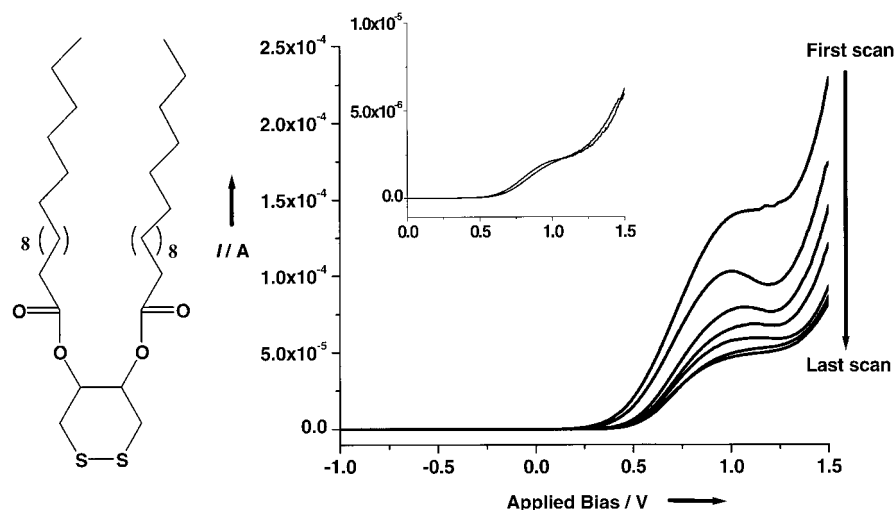


Figure 3.  $I$ – $V$  curves of a device, made with molecules similar to those used for Figure 1, but with long aliphatic chains (left). These molecules pack in a relatively ordered monolayer. After some initial degradation in their  $I$ – $V$  curves, such devices show stable “NDR-like” characteristics as can be seen in the insert, which shows the  $I$ – $V$  curves of a device under continuous cycling.

The above results suggest a new mechanism for controllable NDR in molecule-controlled devices. The diversity of electro-switchable dipole molecules that can be prepared makes this new approach a promising tool for tailor-made NDR devices.

Received: September 21, 2001 [Z17945]

- [1] L. Esaki, *Phys. Rev.* **1958**, 109, 603.
- [2] S. M. Sze, *Physics of Semiconductor Devices*, 2 ed., Wiley, New York, **1981**.
- [3] *Molecular Electronics: Science and Technology* (Eds.: A. Aviram, M. Ratner), New York Academy of Sciences, New York, **1998**.
- [4] Y. Q. Xue, S. Datta, S. Hong, R. Reifenberger, J. I. Henderson, C. P. Kubiak, *Phys. Rev. B* **1999**, 59, R7852.
- [5] C. G. Zeng, H. Q. Wang, B. Wang, J. L. Yang, J. G. Hou, *App. Phys. Lett.* **2000**, 77, 3595.
- [6] J. Gaudio, L. J. Lauhon, W. Ho, *Phys. Rev. Lett.* **2000**, 85, 1918.
- [7] J. Chen, M. A. Reed, A. M. Rawlett, J. M. Tour, *Science* **1999**, 286, 1550.
- [8] J. M. Seminario, A. G. Zacarias, J. M. Tour, *J. Am. Chem. Soc.* **2000**, 122, 3015.
- [9] J. Chen, W. Wang, M. A. Reed, A. M. Rawlett, D. W. Price, J. M. Tour, *App. Phys. Lett.* **2000**, 77, 1224.
- [10] M. A. Reed, J. Chen, A. M. Rawlett, D. W. Price, J. M. Tour, *App. Phys. Lett.* **2001**, 78, 3735.
- [11] M. T. Stankovitch, A. J. Bard, *J. Electroanal. Chem.* **1977**, 75, 487.
- [12] K. Slowinski, H. K. Y. Fong, M. Majda, *J. Am. Chem. Soc.* **1999**, 121, 7257.
- [13] K. Slowinski, M. Majda, *J. Electroanal. Chem.* **2000**, 491, 139.
- [14] R. E. Holmlin, R. Haag, M. L. Chabinyc, R. F. Ismagilov, A. E. Cohen, A. Terfort, M. A. Rampi, G. M. Whitesides, *J. Am. Chem. Soc.* **2001**, 123, 5075.
- [15] R. E. Holmlin, R. F. Ismagilov, R. Haag, V. Mujica, M. A. Ratner, M. A. Rampi, G. M. Whitesides, *Angew. Chem.* **2001**, 113, 2378; *Angew. Chem. Int. Ed.* **2001**, 40, 2316.
- [16] M. Wittmer, J. L. Freeouf, *Phys. Rev. Lett.* **1992**, 69, 2701.
- [17] M. Bruening, R. Cohen, J. F. Guillemoles, T. Moav, J. Libman, A. Shanzer, D. Cahen, *J. Am. Chem. Soc.* **1997**, 119, 5720.
- [18] A. Vilan, A. Shanzer, D. Cahen, *Nature* **2000**, 404, 166.
- [19] Y. Selzer, D. Cahen, *Adv. Mater.* **2001**, 13, 508.
- [20] D.-G. Wu, J. Ghabboun, J. L. Martin, D. Cahen, *J. Phys. Chem. B* **2001**, 105, 12011.
- [21] H. Rhoderick, *Metal-Semiconductor Contacts*, Oxford Press, Oxford, **1980**.
- [22] H. O. Finklea in *Electroanalytical chemistry*, Vol. 19 (Eds.: A. J. Bard, I. Rubinstein), Marcel Dekker, New York, **1996**.
- [23] Geometry optimization of the dianionic molecules resulted in chemically unreasonable structures because of repulsion between the negatively charged S termini. To circumvent this problem, calculations were made on “half” of the molecules, that is, on the  $\text{XC}_6\text{H}_5(\text{CO})\text{CH}_2\text{CH}_2\text{S}^-$  ( $\text{X} = \text{CF}_3$ ,  $\text{CN}$ ,  $\text{H}$ ,  $\text{CH}_3\text{O}$ ) parts. Starting geometries were obtained using the PM3 semiempirical method (J. J. P. Stewart, *J. Comput. Chem.* **1989**, 10, 209); further optimizations were carried out using the B3LYP density functional method (A. D. Becke, *J. Chem. Phys.* **1993**, 98, 5648; C. Lee, W. Yang, R. G. Parr, *Phys. Rev. B* **1988**, 37, 785) with the aug-cc-pVDZ basis set (R. A. Kendall, T. H. Dunning, Jr., R. J. Harrison, *J. Chem. Phys.* **1992**, 96, 6796).  $C_s$  symmetry was imposed throughout. All calculations were carried out using the Gaussian 98 program system (Gaussian 98 (Revision A.7), M. J. Frisch, G. W. Trucks, H. B. Schlegel, G. E. Scuseria, M. A. Robb, J. R. Cheeseman, V. G. Zakrzewski, J. A. Montgomery, R. E. Stratmann, J. C. Burant, S. Dapprich, J. M. Millam, A. D. Daniels, K. N. Kudin, M. C. Strain, O. Farkas, J. Tomasi, V. Barone, M. Cossi, R. Cammi, B. Mennucci, C. Pomelli, C. Adamo, S. Clifford, J. Ochterski, G. A. Petersson, P. Y. Ayala, Q. Cui, K. Morokuma, D. K. Malick, A. D. Rabuck, K. Raghavachari, J. B. Foresman, J. Cioslowski, J. V. Ortiz, B. B. Stefanov, G. Liu, A. Liashenko, P. Piskorz, I. Komaromi, R. Gomperts, R. L. Martin, D. J. Fox, T. Keith, M. A. Al-Laham, C. Y. Peng, A. Nanayakkara, C. Gonzalez, M. Challacombe, P. M. W. Gill, B. G. Johnson, W. Chen, M. W. Wong, J. L. Andres, M. Head-Gordon, E. S. Replogle, J. A. Pople, Gaussian, Inc., Pittsburgh, PA, **1998**).
- [24] S. Datta, W. D. Tian, S. H. Hong, R. Reifenberger, J. I. Henderson, C. P. Kubiak, *Phys. Rev. Lett.* **1997**, 79, 2530.
- [25] V. Mujica, A. E. Roitberg, M. Ratner, *J. Chem. Phys.* **2000**, 112, 6834.
- [26] Y. Xue, S. Datta, M. A. Ratner, *J. Chem. Phys.* **2001**, 115, 4292.
- [27] N. D. Lang, Ph. Avouris, *Phys. Rev. Lett.* **2000**, 84, 358.
- [28] E. Laviron in *Electroanalytical chemistry*, Vol. 12 (Ed.: A. J. Bard), Marcel Dekker, New York, **1982**.
- [29] Upon adsorption, this gap is expected to decrease to about half of this value; see T. Vondrak, C. J. Cramer, X.-Y. Zhu, *J. Phys. Chem. B* **1999**, 103, 8915.
- [30] In earlier experiments with the same molecules we investigated similar junctions ( $\text{Au}/\text{molecule}/\text{SiO}_2/\text{Si}$ ) as a function of temperature, so as to separate the rectification signature that arises from the molecules from that which arises from the Schottky interface.<sup>[19]</sup> In such junctions no redox chemistry occurs as the S–S bond is cleaved as part of the adsorption process on Au.<sup>[22]</sup> The electron tunneling parameters extracted there, which are similar to those we find near zero bias for hole tunneling through long alkyl thiols in the present junctions (unpublished results), were used in this study.
- [31] J. P. Kirby, J. A. Roberts, D. G. Nocera, *J. Am. Chem. Soc.* **1997**, 119, 9230.
- [32] M. A. Fox, *Acc. Chem. Res.* **1999**, 32, 201.
- [33] The devices, with the exception of the ones described in Figure 3, show hysteresis between the forward and reverse scan. This behavior is expected considering that the molecules switch between neutral and charged forms. It agrees also with Laviron’s theory<sup>[28]</sup> according to which no reverse peak is expected (in the potential range of the forward peak) if the kinetics of the process are slow.
- [34] C. P. Collier, G. Mattersteig, E. W. Wong, Y. Luo, K. Beverly, J. Sampaio, F. M. Raymo, J. F. Stoddart, J. R. Heath, *Science* **2000**, 289, 1172.